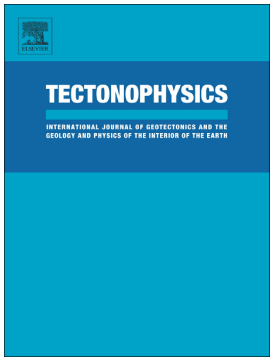

Active tectonics in the Gulf of California and seismicity (M>3.0) for the period 2002–2014

R.R. Castro, J.M. Stock, E. Hauksson, R.W. Clayton

PII: S0040-1951(17)30070-7
DOI: doi: 10.1016/j.tecto.2017.02.015
Reference: TECTO 127407

To appear in: *Tectonophysics*

Received date: 29 July 2016
Revised date: 14 February 2017
Accepted date: 20 February 2017

Please cite this article as: R.R. Castro, J.M. Stock, E. Hauksson, R.W. Clayton , Active tectonics in the Gulf of California and seismicity (M>3.0) for the period 2002–2014. The address for the corresponding author was captured as affiliation for all authors. Please check if appropriate. Tecto(2017), doi: 10.1016/j.tecto.2017.02.015

ACTIVE TECTONICS IN THE GULF OF CALIFORNIA AND SEISMICITY (M>3.0) FOR THE PERIOD 2002-2014

Castro R.R.[1], J.M. Stock[2], E. Hauksson[2], and R.W.Clayton[2]

[1] *Centro de Investigación Científica y de Educación Superior de Ensenada (CICESE), División Ciencias de la Tierra, Departamento de Sismología, Carretera Tijuana-Ensenada No. 3918, 22860 Ensenada, Baja California, México.*

[2] *California Institute of Technology, Seismological Laboratory, 1200 E. California Blvd., Pasadena CA 91125, U.S.A.*

***Keywords**:* Seismotectonics; Gulf of California, Mexico; Seismicity catalog.

A B S T R A C T

We present a catalog of accurate epicenter coordinates of earthquakes located in the Gulf of California (GoC) in the period 2002-2014 that permits us to analyze the seismotectonics and to estimate the depth of the seismogenic zone of this region. For the period April 2002 to December 2014 we use body-wave arrival times from regional stations of the Broadband Seismological Network of the GoC (RESBAN) operated by CICESE to improve hypocenter locations reported by global catalogs. For the northern region of the GoC (30°N – 32°N) we added relocated events from the 2011-Hauksson-Yang-Shearer, Waveform Relocated Earthquake Catalog for Southern California (Hauksson *et al*., 2012; Lin *et al*., 2007). From October 2005 to October 2006 we incorporated hypcenters located by Sumy *et al*. (2013) in the southern GoC combining an array of ocean-bottom seismographs, of the SCOOBA experiment, with onshore stations of the NARS-Baja array. This well constrained catalog of seismicity highlights zones of active tectonics and seismic deformation within the North America-Pacific plate boundary. We estimate that the minimum magnitude of completeness of this catalog is Mc=3.3±0.1 and the b = 0.92±0.04 value of the Gutenberg-Richter relation. We find that most earthquakes in the southern GoC are generated by transform faults and this region is more active than the central GoC region. However, the northern region, where most deformation is generated by oblique faults is as active as the southern region. We used the ISC catalog to evaluate the size distribution of seismicity of these regions, and the b value of the Gutenberg-Richter relation and found that b is slightly lower in the central GoC (b=0.86±0.02) compared to the northern (b=1.14±0.04) and the southern (b=1.11±0.04) regions. We observed seismicity that occurs in the Stable Central Peninsular Province, despite the fact that significant active deformation has not been identified in this region.

1. Introduction

The Gulf of California (GoC) contains an active fault system that connects the San Andreas Fault to the north with the East Pacific Rise to the south. The seismicity in the GoC is mostly governed by large transform faults linked by extensional basins (Lonsdale, 1989; Stock and Hodges, 1989). Most earthquakes near these transform faults are right lateral strike-slip events, and normal fault events tend to occur on the spreading centers (Goff *et al*., 1987). The seismicity of the GoC has been previously studied using global catalogs of earthquakes (e.g. Sykes, 1968, 1970; Molnar, 1973; Goff *et al*., 1987) and a few with regional stations (Lomnitz *et al*., 1970; Thatcher and Brune, 1971; Reid *et al*., 1973; Reichle and Reid, 1977). More recently, Castro *et al*., (2011) relocated small- to moderate-sized earthquakes in the GoC that occurred from April 2002 to August 2006. For the period from October 2005 to October 2006 Sumy *et al*., (2013) located the seismicity in the southern GoC using an array of ocean-bottom seismographs, of the SCOOBA (Sea of Cortez Ocean-Bottom Array) experiment, combined with onshore stations of the NARS-Baja array (Network of Autonomously Recording Seismographs) (Trampert *et al*., 2003; Clayton *et al*., 2004). These earthquake catalogs of well-constrained epicenters have permitted a more detailed visualization of the shape of the Pacific-North America plate boundary and yield a better understanding of the kinematics of seafloor spreading and continental extension within the GoC. The regional catalogs also provide new evidence for extensional deformation near the spreading centers and within the basins of the GoC (Sumy *et al*., 2013).

In this paper we compile a catalog of accurately located earthquakes of the GoC region for the period 2002-2014, including some of the previously mentioned studies as well as new work. We use body-wave arrival times from regional stations of the Broadband Seismological Network of the GoC (RESBAN) operated by CICESE (*Centro de Investigación Científica y de Educación*

Superior de Ensenada, Baja California) to relocate 2850 events reported by the International Seismological Centre (ISC) in the GoC. For the northern GoC (30°N -32°N) we include in the catalog earthquakes from the 2011- Hauksson-Yang-Shearer, Waveform Relocated Earthquake Catalog for Southern California (Hauksson *et al*., 2012; Lin *et al*., 2007). We used for the period October 2005 to October 2006 hypocenters located by Sumy *et al*. (2013) in the central-southern GoC from earthquakes recorded by the array of ocean-bottom seismographs, of the SCOOBA experiment, combined with onshore stations of the NARS-Baja array. The new catalog presented here is an improvement of hypocenter locations within the GoC reported by global catalogs. Note that the catalog does not include all events, because if an event did not pass our selection criteria for location accuracy, we did not include it. This provides us clearer picture of the distribution of the seismicity than if we used all the events in this region from regional or global catalogs.

1.1 Geological setting

The Gulf of California is a trans-tensional rift system located between the Sierra Madre Occidental of continental Mexico and the narrow Peninsular Ranges of Baja California (Fig. 1). The peninsula of Baja California moves almost completely with the Pacific plate at a rate of approximately 48 mm yr^{-1} across the GoC (DeMets and Dixon 1999; Dixon *et al*., 2000). Relative motion between the Baja California peninsula and the Pacific plate is suggested to be less than 3 mm/yr (DeMets *et al*., 2010) and modeling of geodetic data across the plate boundary, at the Ballenas Channel, gives a slip rate of 47.3 +/_ 0.8 mm/yr (Plattner *et al*., 2015). The Pacific-North America plate boundary has undergone a major reorganization, from oblique convergence with the Farallon plate to trans-tensional shearing, since ~12Ma, after the southward migration of the Rivera triple junction (Atwater, 1970; Stock and Hodges, 1989). At

the present time, the boundary between the Pacific and -North America plates consists of short, nascent ridge centers connected by transform faults (Thatcher and Brune, 1971). Faulting in the GoC is dominated by right-lateral strike-slip motion on the transform faults that link spreading centers. In the southern GoC the spreading centers are well-developed ridge segments whereas in the northern GoC these are sedimentary pull-apart basins (Moore, 1973; Lonsdale, 1985).

1.2. Regional broadband arrays

The NARS-Baja array (Trampert *et al*., 2003; Clayton *et al*., 2004) operated from the spring of 2002 to the fall of 2008. This seismic network consisted of 14 broadband stations from Utrecht University (Fig. 1), with STS2 sensors, a 24-bit data logger and a global positioning system. This array was installed and operated in collaboration with the California Institute of Technology, Utrecht University and CICESE. The RESBAN network, started in 1995 with installation of the first two stations (BAHB and GUYB); other stations were installed in later years (Rebollar *et al*., 2001). The seismographs of the RESBAN array are 24-bit Guralp digitizers with sensors Guralp CMG-40T or CMG-3ESP, a CMG-SAM2 acquisition module and GPS for time control. The stations of both arrays record at 20 samples per second, continuously. After the stations of the NARS-Baja array were removed in 2008, RESBAN installed seismographs at former NARS-Baja locations NE79, NE80, NE81 and NE82. At the present time RESBAN operates 13 stations in the GoC region.

The SCOOBA ocean-bottom array comprised 15 OBS seismographs that operated in the southern GoC from October 2005 to October 2006, but only eight stations provided usable data (Sumy *et al*., 2013). The stations of this array consist of four-component broadband instruments from the Scripps Institution of Oceanography that record at 32.25 samples per second.

2. The 2011-Hauksson-Yang-Shearer Catalog for Southern California

This catalog consists of relocated earthquakes recorded by the Southern California Seismic Network (SCSN) from 1981 through June 2011 (Hauksson *et al*., 2012). The catalog contains events in the region extending from Owens Valley in the north and Baja California in the south, and the magnitudes of the earthquakes reported range from M 0.0 to 7.3.

Hauksson *et al*. (2012) used 1D and 3D velocity models from Hauksson (2000) to improve the locations reported in the SCSN catalog. Then, they relocated the hypocenters by clustering the events and using differential travel times to determine relative locations within each cluster (e.g. Lin *et al*., 2007). They included up to 150 nearest neighbors for the cross-correlation calculation and required that pairs of earthquakes be separated by no more than 2.5 km.

They relocated the hypocenters using multicore central processing units by dividing the region into polygons. They used the clustering method by Shearer *et al*. (2005) and Lin *et al*. (2007) to identify clusters of earthquakes. Then, they used the cross-correlation differential times to relocate the events. The preferred hypocenter locations of this catalog are those determined with travel-time picks and differential travel times. If differential travel-times were not available, they reported hypocenters determined with the 3D velocity model. When these were not available, they included hypocenters determined with HIPOINVERSE-2000 (Klein, 2002) and a 1D velocity model.

Most events (75.3 %) in this catalog were determined with differential travel-times and only 0.3 % were relocated with a 1D model. The earthquake depths in this catalog extend from 0.8 km to about 20 km and only a few events have depths ~30 km.

The 90% of the horizontal location errors are less than 0.75 km and vertical errors are less than 1.25 km.

3. The 2013-Sumy *et al*. Catalog for the Southern Gulf of California

Sumy *et al*. (2013) used *P*-wave pick arrivals, automatically detected and manually inspected, to locate hypocenters in the southern Gulf of California with the HIPOINVERSE-2000 (Klein, 2002). The data set comes from 8 ocean-bottom seismographs deployed from October 2005 to October 2006 in the southern GoC and 16 broadband seismographs of the NARS-Baja array (Trampert *et al*., 2003; Clayton *et al*., 2004).

They initially located events with four or more *P*-wave picks using a 1D velocity model obtained through a simultaneous inversion using the VELEST algorithm (Kissling, 1988; Kissling *et al*., 1994). To improve the hypocenter locations, they formed seven geographically distinct clusters and relocated the events using the double-difference algorithm by Waldhauser and Ellsworth (2000) and Waldhauser (2001). The mean horizontal location errors, estimated from a bootstrap error analysis, are on the order of ~2km.

4. The International Seismological Centre (ISC) Catalog

We searched in the ISC Bulletin for earthquakes located in the GoC region between 2002-04-01 and 2014-12-31. We found a total of 2850 events (Fig. 1). Most of the earthquakes seem to concentrate in the north and south ends of GoC, and in the Guaymas basin (27°N-28.5°N). The earthquakes in the southern end are typically generated by transform faults and this region is

usually regarded as being more active than the northern GoC region, where most deformation is generated by oblique faults. We quantify the rate of seismicity of these regions, and the amount of seismic activity with the Gutenberg-Richter (G-R) relation.

We divided the GoC region into four zones (30°N-32°N, 28°N-30°N, 26°N-28°N and 23°N-26°N) and calculated the number of events and the cumulative number for the magnitude range 0.1-7.0, with magnitude increments of 0.1. Fig. 2 displays the frequency-magnitude distributions of the four zones. The distribution of non-cumulative number of events (circles in Fig.2) is useful to identify the minimum magnitude of completeness (*Mc*) of the catalog (e.g. Wiemer and Wyss, 2000; Zúñiga and Castro, 2005). We found that *Mc* varies between 3.5±0.1 and 3.6±0.1, being 3.5±0.1 for the central GoC and 3.6±0.1 for the north and south zones. We also calculated the *b* value of the G-R law (solid lines in Fig. 2) for the four zones. The most northern zone (32°N-30°N) has the larger number of events (950), for the period analyzed, and similar *b* value (*b*=1.14±0.04) than the southern zone (26°N-23°N) (*b*=1.11±0.04). The north-central zone (30°N-28°N) has the smallest number of events (384) and the smallest *b* value (*b*=0.86±0.02) of the four zones.

5. Hypocentral Locations from Regional Data

Earthquake locations based on regional body-wave arrivals usually provide better hypocentral coordinates than global catalogs. For instance, Castro *et al*. (2011a) found that earthquakes with *mb* magnitude 3.2-5.0 in the GoC reported by the Preliminary Determination of Epicenters (PDE) catalog differ on the average by as much as ~40 km from those located with regional data. They also found that the epicentral location discrepancies decrease for larger

earthquakes (*Mw*5-6.7) to approximately 25 km but these differences are still important. Sumy *et al*. (2013) compared the epicentral locations of earthquakes in the southern GoC obtained with regional data with those in the ISC catalog and found that the epicenters differ by an average of ~50 km.

In this paper we estimated initial hypocentral locations using handpicked *P* and *S* wave arrival times, with an approximate accuracy of one tenth of a second, from the regional stations of RESBAN (Fig. 1) and the HYPOINVERSE computer code (Klein, 2002). We selected events in the GoC, from the global catalog, that occurred between 2002 and 2014 and were recorded by at least four stations of RESBAN. We used a four layer velocity model determined by Lopez-Pineda *et al*. (2007) from surface-wave analysis. The *P*-wave velocity of this model varies from 4.6 to 7.9 km/s for the first 25 km, and has a velocity of 8.2 km/s for the upper mantle (dotted line in Fig. 3).

6. Relocated Hypocenters

The hypocentral locations obtained with HYPOINVERSE were relocated using the Source Specific Station Term (SSST) method (Richards-Dinger and Shearer, 2000; Lin and Shearer, 2005) and the Double Difference (hypoDD) algorithm (Waldhauser and Ellsworth, 2000). The SSST method accounts for lateral heterogeneities of the velocity structure calculating specific station terms of each target event. In this technique each station has a correction function that varies with earthquake position. Lin and Shearer (2005) implemented the SSST technique in their COMPLOC earthquake location code. We used a version of this computer code that uses

regional phases and weights the arrival times according to the hypocentral distance (e.g. Castro, Shearer, *et al*., 2010).

We divided the GoC region into nine boxes (Fig. 1) taking into account the distribution of epicenters located with HYPOINVERSE. We used arrival times from all the available stations but only earthquakes within the corresponding box of the target event to calculate the SSST correction. We tested the three models shown in Fig. 3 and compare the root mean square (RMS) of the residual travel times to select the best model. The velocity model of Gonzalez-Fernandez *et al*. (2005) (solid line in Fig. 3) was determined from a 280km-long multi-channel seismic reflection line deployed in the northern GoC. This four-layer model includes an uppermost layer with *P*-wave velocities between 1.77 and 2.15 km/s that represent the sediments. The second velocity layer (4.11-5.09 km/s) corresponds to more deeply bury sedimentary rocks. The middle crust has velocities of 5.37-5.67 km/s, the lower crust 6.58-6.73 km/s and the upper mantle a velocity of 7.9 km/s. In a previous study Castro *et al*. (2011a) tested this and other three models proposed for the GoC and found that the model obtained by Gonzalez-Fernandez *et al*. (2005) (Model GF2005 henceforth) gives the smallest residuals. Sumy *et al*. (2013) determined a velocity model (dashed line in Fig.3) inverting arrival times from 228 earthquakes using the VELEST algorithm (Kissling, 1988; Kissling *et al*., 1994). This model is similar to the model of Lopez-Pineda *et al*. (2007) (dotted line in Fig. 3). We also relocated the events with Sumy *et al*. (2013) model and obtained similar results as with the GF2005 model. We decided to use the GF2005 model for the rest of the analysis.

We also used the hypoDD code (Waldhauser and Ellsworth, 2000) to relocate the earthquakes initially located with HYPOINVERSE. The Double Difference (DD) method uses pairs of nearby earthquakes with small hypocentral separation compared to the source-station

distance and the expected scale length of the velocity heterogeneities. Thus, the difference in the observed travel times of the two events at a given station is attributed to the spatial offset between them and can be calculated accurately.

We first used the PH2DT code (Waldhauser and Ellsworth, 2000) to form travel time differences from *P*- and *S* wave picks and then hypoDD to relocate the initial epicenters. The maximum distance between source pair and stations was limited to 800 km, the maximum hypocentral separation to 20 km, and the maximum number of links per event to 150. We relocated the earthquakes by dividing the GoC region into the same nine boxes as before. A few events (Table 1) have a resulting focal depth greater than 20 km. We revised the hypocentral locations of these events and found that the focal depths obtained with the SSST method are shallower for many of those events and the vertical error, estimated with HYPOINVERSE, significant (erz >10 km). We decided to keep these events in the catalog (Table S1) because the horizontal error is small but we did not use them to analyze the cross sections. Fig. 4 (left frame) shows the distribution of the hypocenters relocated with the DD algorithm, projected on a plane parallel to the axis of the GoC (NW-SE direction) using as origin the northernmost point of the Gulf (31.786^0N,114.750^0W) (profile A-A' in Fig. 1). Most of the earthquakes have focal depths less than 10 km and the deepest are located on the northwestern side of the GoC. We also projected the hypocenters on a plane perpendicular to the GoC axis (Fig. 4 right frame), in the SW-NE direction (profile B-B' in Fig. 1). We observed in this projection that earthquakes located near the axis, near zero distance, tend to be shallower than more distant events from the origin, on both SW and NE directions. This variation of focal depth is likely related to the increase of crustal thickness and the temperature decrement towards the margins of the GoC.

Lin and Shearer (2005) compared these two relative hypocenter location algorithms with synthetic data and found that for regions with distributed seismicity, like the GoC region, the DD and SSST methods give relative locations of comparable accuracy. Fig. 5 shows the RMS travel time residuals obtained with the SSST (left frame) and with the DD (right frame) methods. The RMS is less than 0.5 sec for 62 % of the events relocated with SSST and 68% with DD. For RMS < 0.2 sec the percentage of earthquakes is higher with SSST (31%) than that with DD (9%). However, the percentage of events with RMS< 1.0 sec is 96% with DD and 60% with SSST but the number of earthquakes that we were able to relocate with the SSST algorithm was greater because the number of pairs of events with small hypocentral separation is more limited.

7. Results and Discussion

We formed a catalog of relocated hypocenters putting together earthquakes from: (a) 311 events relocated between 32°N and 30°N in the period 2002-2014 from the 2011- Hauksson-Yang-Shearer, Waveform Relocated Earthquake Catalog for Southern California (Hauksson *et al*., 2012; Lin *et al*., 2007); For this catalog, 90% of the horizontal location errors are less than 0.75 km and the vertical errors less than 1.25 km; When hypocenter coordinates were not available in this catalog we reported our relocation hypocenters; (b) 652 earthquakes located between 29.5°N and 26°N by Sumy *et al*. (2013); The mean horizontal location errors of this catalog, estimated from a bootstrap error analysis, are on the order of ~2km; When hypocenter coordinates were not available, and for the periods June 2002 to September 2005and November 2006 to November 2014 we inserted our hypocenters relocations; and (c) 361 events from our relocations obtained using regional body-wave arrivals for events not located by the former two catalogs. The hypocenter location errors, calculated with Hipoinverse, have a RMS~0.62s and

horizontal error of ~8.6 km. The RMS values of the relocated events were reduced considerably, as shown in Fig. 5. The median value is 0.53 sec and the spatial error of the relocated hypocenters is approximately 2.4 km.

As we discuss in sections 2 and 3, different methods were used to relocate the events of the three catalogs. However, the goal was the same, to determine the best possible hypocenter locations. We combine the three catalogs with the main purpose of understanding the kinematics of seafloor spreading and continental extension within the GoC, and the shape of the Pacific-North America plate boundary. Table S1 of the electronic supplement lists the hypocentral coordinates of the earthquakes compiled. We listed the hypocentral coordinates of earthquakes relocated with the DD algorithm when available, otherwise the coordinates were obtained with the SSST method. Fig. 6 shows the distribution of relocated earthquakes listed in Table S1, and we observe that most epicenters are on the Pacific-North America plate boundary.

We also calculated the minimum magnitude of completeness of the catalog Mc=3.3±0.1 and b= 0.92±0.04 value of the Gutenberg-Richter relation. Fig. 7 shows the cumulative (triangles) and noncumulative (circles) number of events of the catalog of relocated earthquakes and the least-squares fit determined to estimate the b value. The b value of 0.92 is very similar to that obtained (b = 0.86-1.14) for the different regions of the GoC (Fig. 2).

The distribution of focal depths (Fig. 4) can be used to estimate the depth of the seismogenic zone in the GoC. Although most earthquakes have focal depths less than 10 km, events located near the axis of the GoC tend to be shallower. There is a group of events on the southern part of the Baja California Peninsula, near NE78 (Fig. 6) with focal depths above 20 km (Table 1) and another between stations SLGB and BAHB in the vicinity of the Ballenas Transform Fault. These focal depths are beyond the expected bottom of the seismogenic thickness. The crustal

thickness in the Baja California Peninsula varies from approximately 27 km on the western side to ~20 km on the GoC margin. The maximum depth of the Moho of ~ 42 km is beneath the Peninsular Ranges batholith, near the Sierra San Pedro Martir (Reyes *et al*., 2001 and Lewis *et al*., 2001).

7.1. The northern GoC

The northern region of the GoC is characterized by a complex system of faults that strike N-N30^{0}E and are mainly oblique-normal with dips of 60°-80° and small offsets (Persaud *et a*l., 2003). Fig. 8 shows the distribution of the relocated epicenters from the 2011-Hauksson-Yang-Shearer catalog (yellow circles) and other events, not present in that catalog that were relocated using the RESBAN arrival times (red circles). Most events inland (yellow circles) north of the shortline are aftershocks of the 2010 El Mayor-Cucapah (M_w7.2) earthquake. The focal mechanisms (Fig. 8), taken from the GCMT or the NEIC catalog, are from the bigger earthquakes (M_w4.5-5.4) plotted in their relocated positions, and are generally consistent with the NW-SE orientation of the faults located SE of Consag basin. The strike of the fault planes, inferred from the focal mechanisms, are between 45°N and 49°N for events 1 and 2 (Table 2). A set of relocated events near the western margin of the GoC have normal fault mechanism, such as the one we show as event 3 (Fig. 8 and Table 2) which corresponds to an M_w5.2 earthquake that occurred on September 2014. This mechanism is the result of the predominantly tensional stress regime of this region. All five of the events in this swarm have similar focal mechanisms, suggesting active extension along previously unmapped faults near the coastline of Baja California, within extended continental crust of the Gulf of California Extensional Province, west of the Upper Delfin Basin. Shallow fault arrays have been identified in this region by Aragon-

Arreola and Martin-Barajas (2007) although these are mapped parallel to the coastline, not parallel to the nodal planes for the normal faulting focal mechanisms in this swarm. Because this active faulting is part of the overall plate boundary zone, both NE- and NW-striking faults are to be expected as part of the kinematic pattern here.

Based on a simple kinematic analysis Goff *et al*. (1987) suggested that the Delfin and Wagner basins may be part of a triangular pull-apart basin defined by a diffuse zones of extensional faulting previously identified by Henyey and Bischoff (1973). Near the upper Delfin basin (~30.5°N) the seismicity often occurs in the form of large earthquake swarms (e.g. Reichle and Reid, 1977). To the east of the upper Delfin basin the faults change direction, striking predominantly NE-SW. The epicenters coincide with the distribution of the faults and tend to group on the ends of the fractures where is likely that the tectonic stress tends to concentrate.

7.2. The north-central region of the GoC

This region contains the lower Delfin Basin (~30°N) and the Canal de Ballenas (~29°N) (Figure 9). Many of the bigger (M_S > 6) plate boundary earthquakes occur on the transform faults south of Delfin Basin (Goff *et al*., 1987). Important earthquakes have occurred on the Canal de Ballenas Transform Fault. These include, for instance, the earthquakes of 8 July 1975 (M_S 6.5) and 3 August 2009 (M_w6.9), that occurred west of the island Angel de la Guarda. Fig. 9 shows that most of the relocated epicenters are located along the Canal de Ballenas. The bathymetric relief in this zone indicates that a high rate of tectonic activity is currently taking place. The focal mechanisms, taken from the GCMT catalog, are mostly strike-slip with the strike of the fault plane varying between 33°N and 47°N (Table 2) paralleling the strike direction of the Canal de Ballenas fault. The epicenters in black color are the main event (big star) and the aftershocks of

the 2009 earthquake sequence located by Castro *et al*. (2011b) using the SSST technique. Three important aftershocks (smaller stars) with magnitudes m_b 4.9, M_w 6.2 and M_w 5.7 occurred during the first 48 hours after the main event. Castro *et al*. (2011b) estimated that this earthquake sequence had a rupture area of ~600 km^2 and an average slip of 1.3 m. There are several epicenters located on the Stable Central Peninsula Province (SCPP) where significant deformation related to the extension of the gulf has not been identified (Stock *et al*., 1991). These earthquakes are intraplate events probably generated by the stress transferred when the plate boundary ruptures along the Canal de Ballenas Transform fault (Castro *et al*., 2011b). It is possible that these events are reactivating earlier faults, such as the N-S normal faults that bound Bahia de Los Angeles and control topographic steps in the terrain near station BAHB (Figure 9).

East of Angel de la Guarda Island the seismicity is absent. Based on a seismic line that crosses the upper Tiburon basin, offshore of station PLIB, Aragón-Arreola and Martín-Barajas (2007) concluded that that basin is structurally inactive. South of Canal de Ballenas, where en echelon transform zones define the plate boundary, the focal mechanisms of the earthquakes are a combination of strike-slip and normal fault events, and this is another seismically active zone of the GoC (Fig. 9). Gutenberg and Richter (1954) reported an earthquake M=7.5 in this region (28°N, 112.5°W), on the Guaymas Transform fault, that occurred on 16 October, 1907.

7.3. The south-central region of the GoC

The Guaymas and Carmen basins (Fig. 10) are connected by transform faults, where big earthquakes tend to occur, like the 12 March 2003 M_w6.3 event (26.5°N, 110.8°W). The Guaymas basin is considered a narrow and very active magmatic rift (Lizarralde *et al*., 2007). The magmatism in this basin is anomalous with respect to global mid-ocean ridge production

(White *et al*., 1992). Based on wide-angle and multi-channel seismic data, Lizarralde *et al*. (2007) estimated that the continent-ocean transition is located in this basin. Goff *et al*. (1987) found that this transition is also marked by a broader zone of crustal deformation in the north and a ~10° change in the strike of the principal faults on the northern GoC compared with the strike of the main faults in the southern GoC. The earthquakes in this region are distributed in the NW-SE direction along the Guaymas Transform fault. The focal mechanisms show that the strike of the fault plane varies between 35° and 38° (events 9 and 10 in Figure 10 and Table 2). To the south the seismicity changes direction to SW-NE, migrates southeast and connects with the Carmen Transform fault, where the epicenters are distributed again in the NW-SE direction. Gutenberg and Richter (1954) located an *M*=7.0 earthquake on the Carmen Transform fault (27°N, 111°W) that occurred on 27 June 1945. It is interesting to note in Fig. 10 that the number of earthquakes is greater on the NW (~27°N) and SE (~26°10'N) extremes of the Carmen Transform fault, where tectonic stress is presumably higher. We also observed swarms of intraplate events outside of these en echelon structures, on the Peninsula NE of station NE75 and near station NE76, and in the gulf between the step-over of the transform faults. Some of these earthquake swarms in the GoC may be related with magmatic activity that in some cases occur near volcanic seamounts, such as the swarm near (27° N 25', 111° W 50') in Fig. 10. Another set of events, found on land to the NE of station NE75, likely is related to the active faults and geothermal activity at the Tres Virgenes geothermal field, as noted by Sumy *et al*. (2013). High heat flow values obtained offshore in this region of the GoC (Lawver and Williams, 1979) are consistent with active volcanism and hydrothermal venting in the marine basins.

Crustal deformation and seismicity can be related to dynamic processes in the upper mantle. For instance, Di Luccio *et al*. (2014) found prominent low *S*-wave velocity regions near the GoC

rift axis associated with mantle upwelling, and a high-velocity anomaly at 50 km depth extending down to approximately 130 km beneath the Baja California Peninsula, which may be related to the Farallon slab remnant. We plot in Fig. 11 the average *S*-wave velocities obtained by Di Luccio *et al*. (2014) along an east-west profile at 26.8°N together with our relocated earthquakes between 26.7°N and 26.9°N. Romo-Jones (2002) imaged the slab at depths of 30-40 km with a magnetotelluric survey at 28°N across the peninsula. The seismicity near 26.8°N (Fig. 11) is concentrated above the high-velocity region under the Baja California Peninsula. The events located near the Moho, between 10 and 20 km depth, may be related to the slab remnant and the dynamics of the upper mantle. Receiver function results by Persaud *et al*. (2007) near ~27°N, below station NE75 (Fig. 1), suggests a possible slab top close to the Moho, making the upper mantle more rigid than expected. This can explain why some earthquakes may occur below the crust in this region.

7.4. The south region of the GoC

The transform faults south of Carmen basin have also generated important earthquakes in the past, like the 7 January 1901, M_w7.0 (Pacheco and Sykes, 1992). Earthquakes on the Farallon Transform fault follow the NW-SE direction of the strike (Fig. 12), and the distribution of epicenters becomes more diffuse on the southern end, near the rift that connects with the Pescadero Transform fault. This is one of the more seismically active regions in the GoC and the focal mechanisms are predominantly strike-slip as shown in Fig. 12. The strike of the fault planes varies between 37° and 45° (Table 2).

The Alarcon basin, located at the southern end of the GoC, is a wide rift that went through approximately 350 km of continental extension, before seafloor spreading started in this rift

segment 2-3 Myr ago (Lizarralde *et al*., 2007). The earthquakes here align NW-SE along the Alarcon Transform fault (~24°N) and SW-NE at the southern end (Fig. 12). We also observe a swarm of events SW of the transform fault (~23°N 30'), near Seamounts, that could be associated to volcanism, and a few intraplate earthquakes NE of the main fault. These events align in the N-S direction (~108°W 15') and could be related to the bathymetric feature that runs in the same direction.

Fig. 13 shows average *S*-wave velocities along an east-west profile at 25.8°N determined by Di Luccio *et al*. (2014) and a seismicity cross-section that includes our hypocenters relocated between 25.7°N and 25.9°N. Most of these earthquakes are within the GoC, above the high-velocity region imaged by Di Luccio *et al*. (2014), but there are a few events towards the west, under the Stable Central Peninsula Province, where the shear velocity in the upper mantle decreases to ~4.1 km/s. This moderate low-velocity zone may be related to upwelling of asthenospheric material in the upper mantle as suggested by Lizarralde *et al*. (2007) and can be associated to a slab window (Di Luccio *et al*., 2014). The earthquakes in this region may be the result of stress accumulated during these processes. There are a few active faults documented in shallow water of the western margin of the Gulf of California in this region, in the continental crust (Nava-Sanchez *et al*., 2001) but these do not appear to be associated with any significant seismicity during the time interval that we examined in compiling this catalog.

8. Conclusions

We provide a seismotectonic interpretation of a new catalog of seismicity with well constrained hypocenters located in the GoC. This catalog permits us to identify regions of active tectonics within the Pacific-North America plate boundary. We estimate that the minimum magnitude of completeness of this catalog is *Mc=3.3* and the overall *b* value of the Gutenberg-Richter equals 0.92±0.04. We found that the *b* value of 1.14 and the number of events of the southern region of the GoC is larger than other regions, indicating that this region is the most seismically active of the gulf. Although most events in the catalog are located on the plate boundary, stress transfer outside the boundary caused by geometrical irregularities and/or reactivation of preexisting faults, generates clustered swarms of intraplate earthquakes. Such seismicity occurred in the Stable Central Peninsula Province (Figs. 9 and 10) despite the fact that significant active deformation related to the extension of the GoC has not been identified in that province (Stock *et al*., 1991).

Acknowledgments

This paper was prepared while the first author (RRC) was on sabbatical year in Caltech. We thank CONACYT and Prof. Michael Gurnis for the support provided. The operation of the RESBAN network has been possible thanks to the financial support of the Mexican National Council for Science and Technology (CONACYT) (projects CB-2011-01-165401(C0C059), G33102-T and 59216). Antonio Mendoza Camberos pre-process the data from the RESBAN network and Arturo Perez Vertti maintains and operates the stations. The authors thank the editors and the comments and suggestions of two anonymous reviewers.

References

Aragón-Arreola, M. and A. Martin-Barajas (2007). Westward migration of extension in the northern Gulf of California, Mexico, *Geology*, 35, 571-574.

Atwater, T. (1970). Implications of plate tectonics for the Cenozoic tectonic evolution of western North America, *Geol. Soc. Am.*, 81, 3513-3536.

Castro, R.R., P.M. Shearer, L. Astiz, M. Suter, C. Jacques-Ayala, and F. Vernon (2010). The Long-lasting Aftershock Series of the 3 May 1887 M_W 7.5 Sonora Earthquake in the Mexican Basin and Range Province, *Bull. Seism. Soc. Am*., 100, 1153-1164.

Castro, R.R., A. Pérez-Vertti, I. Mendez, A. Mendoza, and L. Inzunza (2011a). Location of moderate size earthquakes recorded by the NARS-Baja array in the Gulf of California region between 2002 and 2006. *Pure Appl. Geophys.*, 168, 1279-1292, DOI 10.1007/s00024-010-0177-y.

Castro, R.R., C.M. Valdés-Gonzalez, P.M. Shearer, V. Wong, L. Astiz, F. Vernon, A. Pérez-Vertti and A. Mendoza (2011). The August 3, 2009 Canal de Ballenas region, Gulf of California earthquake, (Mw6.9) and the aftershocks, *Bull. Seism. Soc. Am.*, **101**, 929-939.

Clayton, R. W., J. Trampert, C. J. Rebollar, J. Ritsema, P. Persaud, H. Paulssen, X. Pérez-Campos, A. van Wettum, A. Pérez-Vertti, and F. diLuccio, (2004). The NARS-Baja array in the Gulf of California Rift Zone, *Margins Newsletter 13*, 1-4.

DeMets, C., and T.H. Dixon (1999). New kinematic models for Pacific-North America motion from 3 Ma to present. I. Evidence for steady motion and biases in the NUVEL-1A model, *Geophys. Res. Lett*. 26, 1921-1924.

DeMets, C., R.G. Gordon, D.F. Argus (2010). Geologically current plate motions, *Geophys. J. Int.*, 181, 1-80. Doi:10.1111/j.1365-246X.2009.04491.x

Di Luccio, F., P. Persaud, and R.W. Clayton (2014). Seismic structure beneath the Gulf of California: a contribution from group velocity measurements, *Geophys. J. Int*., 199, 1861-1877.

Dixon, T.H., F. Farina, C. DeMets, F. Suarez-Vidal, J. Fletcher, B. Marquez-Azua, M. Miller, O. Sanchez, and P.J. Umhoefer (2000). New kinematic models for Pacific-North America motion from 3 Ma to present. II. Evidence for a "Baja California shear zone*", Geophys. Res. Lett*., 26, 1921-1924.

Gutenberg, B., and C.F. Richter (1954). *Seismicity of the Earth and associated phenomena*, 2nd ed., 310 pp., Princeton University Press, Princeton, N.J.

Hauksson, E. (2000). Crustal structure and seismicity distributions adjacent to the Pacific and North America plate boundary in Southern California. *J. Geophys. Res*., 105, 13875-13903.

Hauksson, E., W. Yang, and P.M. Shearer (2012). Wave form relocated earthquake catalog for Southern California (1981 to 2011). *Bull. Seism. Soc. Am*., 102, 2239-2244.

Hauksson, E., H. Kanamori, J. Stock, M-H. Cromier and M. Legg (2013). Active Pacific North America Plate boundary tectonics as evidenced by seismicity in the oceanic lithosphere offshore Baja California, Mexico. *Geoph. J. Int*., doi:10.1093/gji/ggt467.

Henyey, T.L., and J.L. Bischoff (1973). Tectonic elements of the northern part of the Gulf of California, *Geol. Soc. Am. Bull*., 84, 315-330.

International Seismological Centre, On-line Bulletin, http://www.isc.ac.uk, *Internatl. Seismol. Cent*., Thatcham, United Kingdom, 2013.

Goff, J.A., E.A. Bergman, and S.C. Solomon (1987). Earthquake Source Mechanism and Transform Fault Tectonics in the Gulf of Californi*a, J. Geophys. Res*., 92, 10,485-10,510.

Gonzalez-Fernandez, A., J.J. Dañobeitia, L.A. Delgado-Argote, F. Michaud, D. Cordoba, and R. Bartolomé (2005). Mode of Extensión and Rifting History of Upper Tiburón and Upper Delfín Basins, Northern Gulf of California, *J. Geophys. Res*., 110, B01313, doi:10.1029/2003JB002941.

Klein, F. W. (2002). User's guide to HYPOINVERSE-2000, a Fortran program to solve for earthquake locations and magnitudes, USGS Open File Report 02-171, 121pp.

Kissling, E. (1988). Geotomography with local earthquake data, *Rev. Geophys*. 26, 659-698.

Kissling, E., W.L. Ellsworth, D. Eberhart-Phillips, and U. Kradolfer (1994). Initial reference models in local earthquake tomography, *J. Geophys. Res*. 99, 19,635-19,646.

Kumar, R.R. and R.G. Gordon (2009). Horizontal thermal contraction of oceanic lithosphere: the ultimate limit to the rigid plate approximation, *J. Geophys. Res*., 114, B01403, doi:10.1029/2007JB005473.

Lawver, L.A., and D.L. Williams (1979). Heat flow in the central Gulf of California, *J. Geophys. Res*., 84, 3465-3478.

Lewis, J.L., S.M. Day, H. Magistrale, R. Castro, L. Astiz, C. Rebollar, J. Eakins, F. Vernon and J.N. Brune (2001). Crustal thickness of the peninsular ranges and gulf extensional province in the Californias, *Jour. of Geophys. Res.,* 106, 13,599-13,611.

Lin, G., and P.M. Shearer (2005). Test of Relative Earthquake Location Techniques Using Synthetic Data, *Jour. Geophys. Res., 110*, B04304, doi:10.1029/2004JB003380.

Lin, G., P.M. Shearer, and E. Hauksson (2007). Applying a three-dimensional velocity model, wave form cross correlation, and cluster analysis to locate southern California seismicity from 1981 to 2005. *J. Geophys. Res*., 112, B12309, doi:10.1029/2007JB004986.

Lizarralde, D., G.J. Axen, H.E. Brown, J.M. Fletcher, A. González-Fernández, A. J. Harding, W.S. Holbrook, G.M. Kent, P. Paramo, and F. Sutherland (2007). Variation in styles of rifting in the Gulf of California, *Nature*, 448, doi:10.1038/nature06035.

Lomnitz, C., F. Mooser, C.R. Allen, J.N. Brune, and W. Thatcher (1970). Seismicity and Tectonics of the Northern Gulf of California Region, Mexico. Preliminary Results, *Geof. Internacional*, 10, 37-48.

Lonsdale, P. (1985). A transform continental margin rich in hydrocarbons, Gulf of California, *Am. Assoc. Pet. Geol. Bull*., 69, 1160-1180.

Lonsdale, P. L. (1989). *Geology and Tectonics History of the Gulf of California*, in The Geology of North America: The Eastern Pacific Ocean and Hawaii, vol. *N*, The Geological Society of America.

López-Pineda, L., C.J. Rebollar, and L. Quintanar (2007). Crustal Thickness Estimates for Baja California, Sonora, and Sinaloa, Mexico, Using Disperse Surface Waves, *J. Geophys. Res*., 112, B04308, doi:10.1029/2005JB003899.

McKenzie, D., J. Jackson, and K. Priestley (2005). Thermal structure of oceanic and continental lithosphere, *Earth planet. Sci. Lett*., 233, 337-349.

Molnar, P. (1973). Fault Plane Solutions of Earthquakes and Direction of Motion in the Gulf of California and on the Rivera Fracture Zone, *Geol. Soc. Am. Bull*., 84, 1651-1658.

Moore, D.G. (1973). Plate-edge deformation and crustal growth, Gulf of California structural province, *Geol. Soc. Am Bull*., 84, 1883-1905.

Nava-Sánchez, E.H., D.S. Gorsline, A. Molina-Cruz (2001). The Baja California peninsula borderland: structural and sedimentological characteristics, *Sedimentary Geology*, 144, 63-82.

Pacheco, J.F. and L.R. Sykes (1992). Seismic Moment Catalog of Large Shallow Earthquakes, 1900 to 1989, *Bull. Seism. Soc. Am*.., 82, 1306-1349.

Persaud, P., J.M. Stock, M.S. Steckler, A. Martin-Barajas, J.B. Diebold, A. Gonzalez-Fernandez, and G.S. Mountain (2003). Active Deformation and Shallow Structure of the Wagner, Consag, andDelfin Basins, Northern Gulf of California, Mexico, *J. Geophys. Res*., *108*(B7), 2355, doi:10,1029/2002JB001937.

Persaud, P., X. Pérez-Campos, and R.W. Clayton (2007). Crustal thickness variations in the margins of the Gulf of California from receiver functions, *Geophys. J. Int*., 170, 687-699.

Plattner, C., R. Malservisi, F. Amelung, T.H. Dixon, M. Hackl, A. Verdecchia, P. Lonsdale, F. Suarez-Vidal, and J. Gonzalez-Garcia (2015). Space geodetic observation of the deformation cycle across the Ballenas Transform, Gulf of California, *J. Geophys. Res. Solid Earth*, 120, 5843-5862.

Rebollar, C.J., L. Quintanar, R.R. Castro, S.M. Day, J. Madrid, J.N. Brune, L. Astiz, and F. Vernon (2001). Source Characteristics of a 5.5 Magnitude earthquake that Occurred in the Transform Fault System of the Delfin Basin in the Gulf of California, *Bull. Seism. Soc. Am*., 91, 781-791.

Reichle, M. and I. Reid, (1977). Detailed Study of Earthquake Swarms from the Gulf of California, *Bull. Seism. Soc. Am*., 67, 159-171.

Reid, I., M. Reichle, J.N. Brune, and H. Bradner, (1973). Microearthquake Studies Using Sonobuoys, Preliminary Results from the Gulf of California, *J. R. Astronom. Soc*., 34, 365-379.

Reyes, L.M., C.J. Rebollar and R. Castro (2001). Depth of the Moho in northern Baja California using (Pg-Pn) travel times, *Geof. Internacional*, 40, 21-29.

Richards-Dinger, K. and P. Shearer (2000). Earthquake Locations in Southern California Obtained Using Source-Specific Station Terms, *Jour. Geophys. Res*., 105, 10,939-10,960.

Romo-Jones, J.M. (2002). Conductividad eléctrica de la litósfera de Baja California en la region de Vizcaino, *PhD thesis*, Centro de Investigación Científica y de Educación Superior de Ensenada (CICESE), 199.

Ryan, W.B.F., S.M. Carbotte, J.O. Coplan, S. O'Hara, A. Melkonian, R. Arko, R.A. Weissel, V. Ferrini, A. Gooswillie, F. Nitsche, J. Bonczkowski, and R. Zemsky (2009). Global multiresolution topography synthesis, *Geochem. Geophys. Geosyst*., 10, Q03014, doi:10.1029/2008GC002332.

Shearer, P., E. Hauksson, and G. Lin (2005). Southern California hypocenter relocation with wave form cross correlation: Part 2, Results using source-specific station terms and cluster analysis, *Bull. Seismol. Soc. Am*. 95, 904-915.

Stock, J.M., and K.V. Hodges (1989). Pre-Pliocene extension around the Gulf of California and the transfer of Baja California to the Pacific Plate, *Tectonics*, 8, 99-115.

Stock, J.M., A. Martin-Barajas, F. Suárez-Vidal and M.M. Miller (1991). Miocene to Holocene extensional tectonics and volcanic stratigraphy of the northeastern Baja California, México, in *Geological Excursions in the Southern California and México*, edited by M.J. Walawender and B.B. Hanan, pp. 44-67, *Geol. Soc. of Am.*, Boulder, Colo.

Sumy, D.F., J.B. Gaherty, W-Y. Kim, T. Diehl, and J.A. Collins (2013). The mechanism of earthquakes and faultingin the southern Gulf of California, *Bull. Seism. Soc. Am*., 103, 487-506.

Sykes, L.R. (1968). Seismological Evidence for Transform Faults, Sea-floor Spreading and Continental Drift, *in the History of the Earth's Crust*, edited by R. A. Phinney, pp. 120-150, Princeton Univ. Press, Princeton, N.J.

Sykes, L.R. (1970). Focal Mechanism Solutions for Earthquakes Along the World Rift System, *Bull. Seismol. Soc. Am*., 60, 1749-1752.

Thatcher, W. and J. N. Brune, (1971). Seismic Study of an Oceanic Ridge Earthquake Swarm in the Gulf of California, *Geophys. J. R. Astron. Soc*., 22, 473-489.

Trampert, J., H. Paulsen, A. Van Wettum, J. Ritsema, R. Clayton, R. Castro**,** C. Rebollar, and A. Pérez-Vertti (2003). New Array Monitors Seismic Activity near the Gulf of California in México, *EOS, Trans. Am. Geoph. Union*, 84, 29-32.

Waldhauser, F., and W.L. Ellsworth (2000). A double-difference earthquake location algorithm: Method and application to the Northern Hayward fault, California, *Bull. Seismol. Soc. Am*. 90, 1353-1368.

Waldhauser, F. (2001). HypoDD- A program to compute double-difference hypocenter locations, *U.S. Geol. Survey, Open-File Rept. 01-113*, 25 pp.

Wessel, P. and W.H.F. Smith, (1998). New, improved version of generic mapping tools released, *Eos Trans*. AGU 79, no. 47, 579.

White, R.S., D. McKenzie, and R.K. O'Nions (1992). Oceanic crust thickness from seismic measurements and rare earth element inversions, *J. Geophys., Res*. 97, 19,683-19,715.

Wiemer, R., and M. Wyss (2000). Minimum magnitude of completeness in earthquake catalogs: examples from Alaska, the western US and Japan, *Bull. Seism. Soc. Am*., 90, 859-869.

Zúñiga, F.R. and R.R. Castro (2005). The RESNOM seismic catalog and its bearing on the seismicity of northwesthern Mexico, *Geof. Internacional*, 44, 143-155.

TABLE 1. Events located with double-difference method (DD) with depths > 20 km. For comparison the depths obtained using the Source Specific Station Term (SSST) method and Hypoinverse (HYPI) are also listed together with the estimate of the vertical error (ERZ).

EVENT	DD Depth in km	SSST Depth in km	HYPI Depth in km	ERZ Error in km
20090803 20:13	22.5	25.9	25.3	95.6
20090803 20:45	41.5	7.2	27.0	43.6
20090803 21:58	39.8	20.7	28.7	42.1
20090803 22:23	41.1	19.0	25.2	99.0
20090803 23:14	21.8	30.0	21.5	82.4
20090803 15:31	41.1	11.5	26.0	86.5
20090805 08:29	44.3	14.4	25.2	99.0
20090805 08:52	41.0	10.6	26.2	86.0
20090805 09:00	42.6	16.7	25.6	98.9
20090803 19:10	21.7	-	19.9	83.0
20090803 23:10	20.5	30.0	20.2	76.3
20090803 23:30	21.3	24.9	24.0	14.3
20090804 01:09	38.0	21.0	23.6	10.0
20090804 15:17	39.4	-	26.4	74.8
20090804 19:21	40.4	13.2	26.1	72.7
20070903 14:46	26.3	-	25.2	23.7

20070913 22:39	28.3	-	26.0	49.7

TABLE 2. Focal-mechanism parameters of selected earthquakes located in the GoC and shown in figures 8-11 (taken from the Global CMT or NEIC catalog). The events are listed from north to south.

Region	No.	Date and Time	Mw	Strike (Deg)	Dip (Deg)	Rake (Deg)
Northern	1	2012/08/27/23:16	5.4	49.0	85.0	-2.0
	2	2012/08/28/13:19	4.5	45.0	89.0	-6.0
	3	2014/09/15/12:23	5.2	32.0	61.0	-73.0
North-Central	4	2009/08/03/17:59	6.9	42.0	85.0	11.0
	5	2009/12/21/08:53	4.8	40.0	60.0	-4.0
	6	2012/04/12/07:05	6.1	42.0	86.0	-30.0
	7	2012/04/12/07:15	7.0	227.0	86.0	22.0
	8	2011/09/10/22:07	4.9	33.0	51.0	-4.0
South-Central	9	2014/08/10/18:46	5.5	215.0	89.0	-1.0
	10	2011/05/24/19:01	5.1	38.0	80.0	-7.0
	11	2007/02/25/01:18	5.2	341.0	29.0	-120.0
	12	2007/02/27/20:08	5.0	353.0	33.0	-88.0
Southern	13	2013/01/13/16:28	5.7	220.0	80.0	3.0
	14	2014/07/22/06:50	5.1	37.0	79.0	-2.0
	15	2013/01/13/17:50	5.4	39.0	83.0	-3.0
	16	2007/03/28/14:28	5.3	39.0	82.0	18.0
	17	2007/03/28/13:21	5.2	217.0	89.0	-10.0
	18	2009/07/03/09:56	5.3	225.0	90.0	5.0
	19	2009/07/03/11:00	5.9	225.0	79.0	9.0
	20	2008/05/05/16:28	4.9	43.0	84.0	2.0
	21	2012/10/08/06:26	6.0	39.0	84.0	-10.0
	22	2007/09/03/03:05	4.9	285.0	67.0	173.0
	23	2007/09/17/00:16	5.4	27.0	78.0	5.0
	24	2007/09/17/08:04	5.0	354.0	54.0	-38.0
	25	2007/09/24/01:49	5.0	359.0	45.0	-40.0

FIGURE CAPTIONS

Figure 1. Location of epicenters (circles) reported by the International Seismological Center (ISC) catalog between 2002-04-01 and 2014-12-31. The triangles are the locations of the broadband seismic stations from the NARS-Baja (NE70 to NE83) and RESBAN (CHXB, BAHB, EVAR, PPXB, PLIB, NOVI, GUYB, NAVO, TOPB, SLGB, SFQB) arrays. The boxes indicate the zones we divided the GoC region for relocation purposes. The lines A-A' and B-B' indicate the cross-section profiles used in Figure 4.

Figure 2. Minimum magnitude of completeness (*Mc*) and *b* value of the ISC catalog for earthquakes located in the GoC between 2002-04-01 and 2014-12-31. The cumulative frequency (triangles) and non-cumulative frequency (circles) from events in four regions of the GoC are displayed. Upper frames correspond to the northern Gulf (latitudes 30°-32°N and 28°-30°N) and bottom frames to the southern GoC (latitudes 26°-28°N and 23°-26°N).

Figure 3. *P* wave velocity models used. The solid line is the model determined by Gonzalez-Fernandez *et al*. (2005), the dotted line is the model of Lopez-Pineda *et al*., (2007) and the dashed line the velocity model derived by Sumy *et al*. (2013).

Figure 4. Cross sections using hypocenters relocated with the double-difference method. The left frame shows the distribution of the earthquakes projected on a plane parallel to the GoC axis (NW-SE direction) with the origin at the northernmost point of the gulf

(31.786°N, 114.750°W) (profile A-A' in Fig. 1). The right frame displays the hypocenters projected on a plane perpendicular to the axis of the gulf, in the SW-NE direction (profile B-B' in Fig. 1). The vertical exaggeration is 60 times the horizontal scale.

Figure 5. Root Mean Squares (RMS) of hypocenter location error versus the percentage of earthquakes located. (a) Using the Source Specific Station Term (SSST) method (Lin and Shearer, 2005). (b) Using the Double-Difference method (Waldhauser and Ellsworth, 2000). We did not include in the catalog any events with RMS>2.

Figure 6. Location of epicenters (circles) listed in Table S1 of the electronic supplement. The topography and bathymetry are from GeoMap App.

Figure 7. Minimum magnitude of completeness (*Mc*) and *b* value of the catalog of relocated earthquakes (shown in Fig. 6) in the GoC region between 2002 and 2014. The cumulative frequency (triangles) and non-cumulative frequency (circles) in the whole GoC region is displayed.

Figure 8. Epicenters relocated in the northernmost zone of the GoC, for the period 2002-2014. The red circles are earthquakes relocated with hypoDD (Waldhauser and Ellsworth, 2000) and the yellow circles are events from the 2011-Hauksson-Yang-Shearer, Waveform Relocated Earthquake Catalog for Southern California (Hauksson *et al*., 2012; Lin *et al*., 2007). The focal mechanisms were taken from the GCMT catalog and the faults from the Generic Mapping Tools (Wessel and Smith, 1998). The topography and bathymetry are from GeoMap App (Ryan *et al*., 2009).

Figure 9. Epicenters relocated in the north-central zone of the GoC, for the period 2002-2014. The red circles are earthquakes relocated with hypoDD (Waldhauser and Ellsworth, 2000) and the yellow circles earthquakes relocated by Sumy *et al*. (2013) using the OBS of the SCOOBA experiment. Epicenters on black were located by Castro *et al*. (2011b) and the focal mechanisms were taken from the GCMT catalog. The topography and bathymetry are from GeoMap App.

Figure 10. Epicenters relocated in the south-central zone of the GoC, for the period 2002-2014. The red circles are earthquakes relocated with hypoDD (Waldhauser and Ellsworth, 2000) and the yellow circles are events located by Sumy *et al*. (2013). The focal mechanisms were taken from the GCMT catalog. The topography and bathymetry are from GeoMap App.

Figure 11. East-west profiles showing the average shear wave velocities (top), modified from Di Luccio *et al*., (2014), and hypocenters relocated in this study between 26.9°N and 26.7°N.

Figure 12. Epicenters relocated in the southern zone of the GoC, for the period 2002-2014. The red circles are earthquakes relocated with hypoDD (Waldhauser and Ellsworth, 2000) and the yellow circles are events located by Sumy *et al*. (2013). The focal mechanisms were taken from the GCMT catalog. The topography and bathymetry are from GeoMap App.

Figure 13. East-west profiles showing the average shear wave velocities (top), modified from Di Luccio *et al*., (2014), and hypocenters relocated in this study between 25.7°N and 25.9°N.

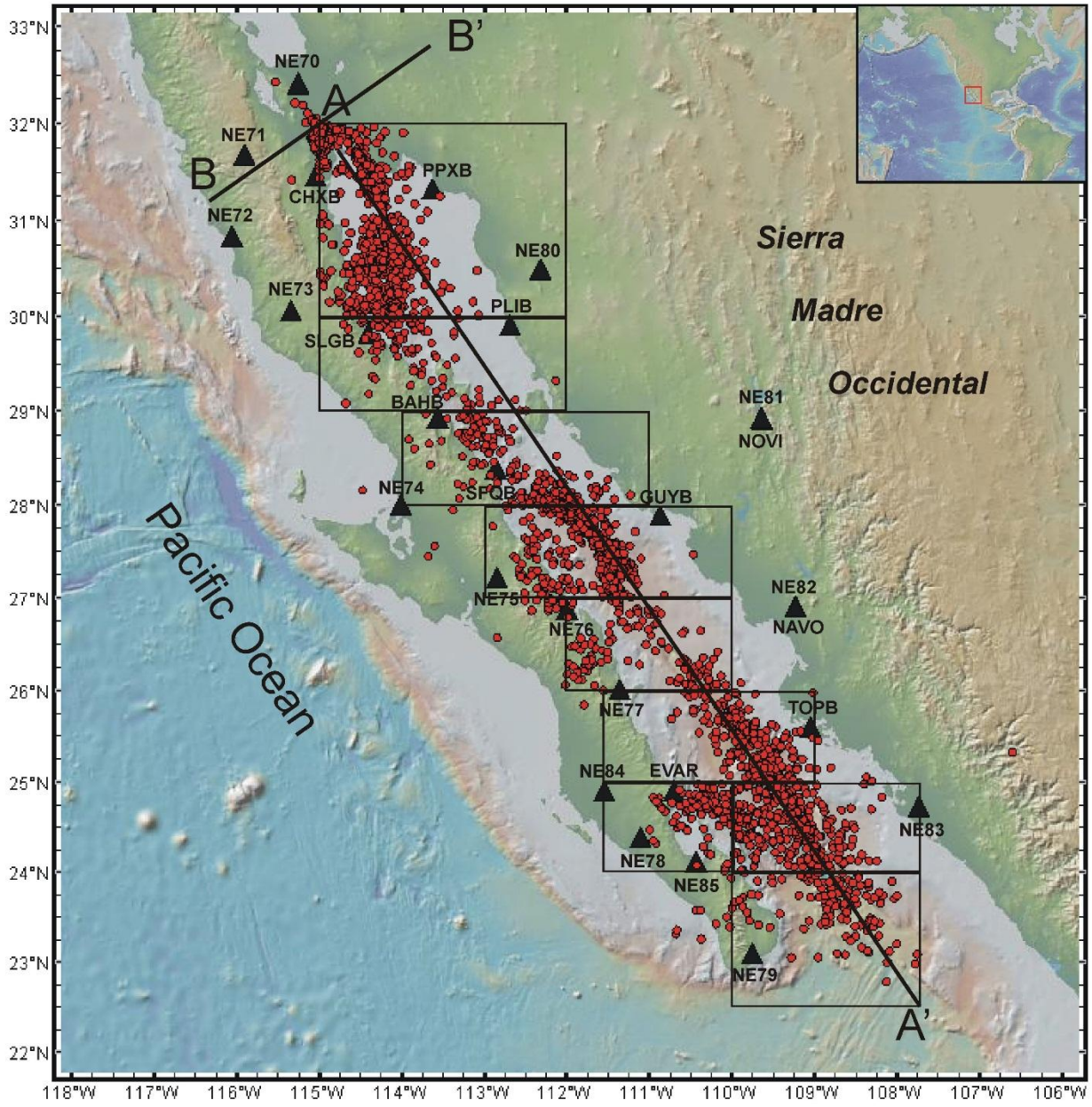

Figure 1. Location of epicenters (circles) reported by the International Seismological Center (ISC) catalog between 2002-04-01 and 2014-12-31. The triangles are the locations of the broadband seismic stations from the NARS-Baja (NE70 to NE83) and RESBAN (CHXB, BAHB, EVAR, PPXB, PLIB, NOVI, GUYB, NAVO, TOPB, SLGB, SFQB) arrays. The boxes indicate the zones we divided the GoC region for relocation purposes. The lines A-A' and B-B' indicate the cross-section profiles used in Figure 4.

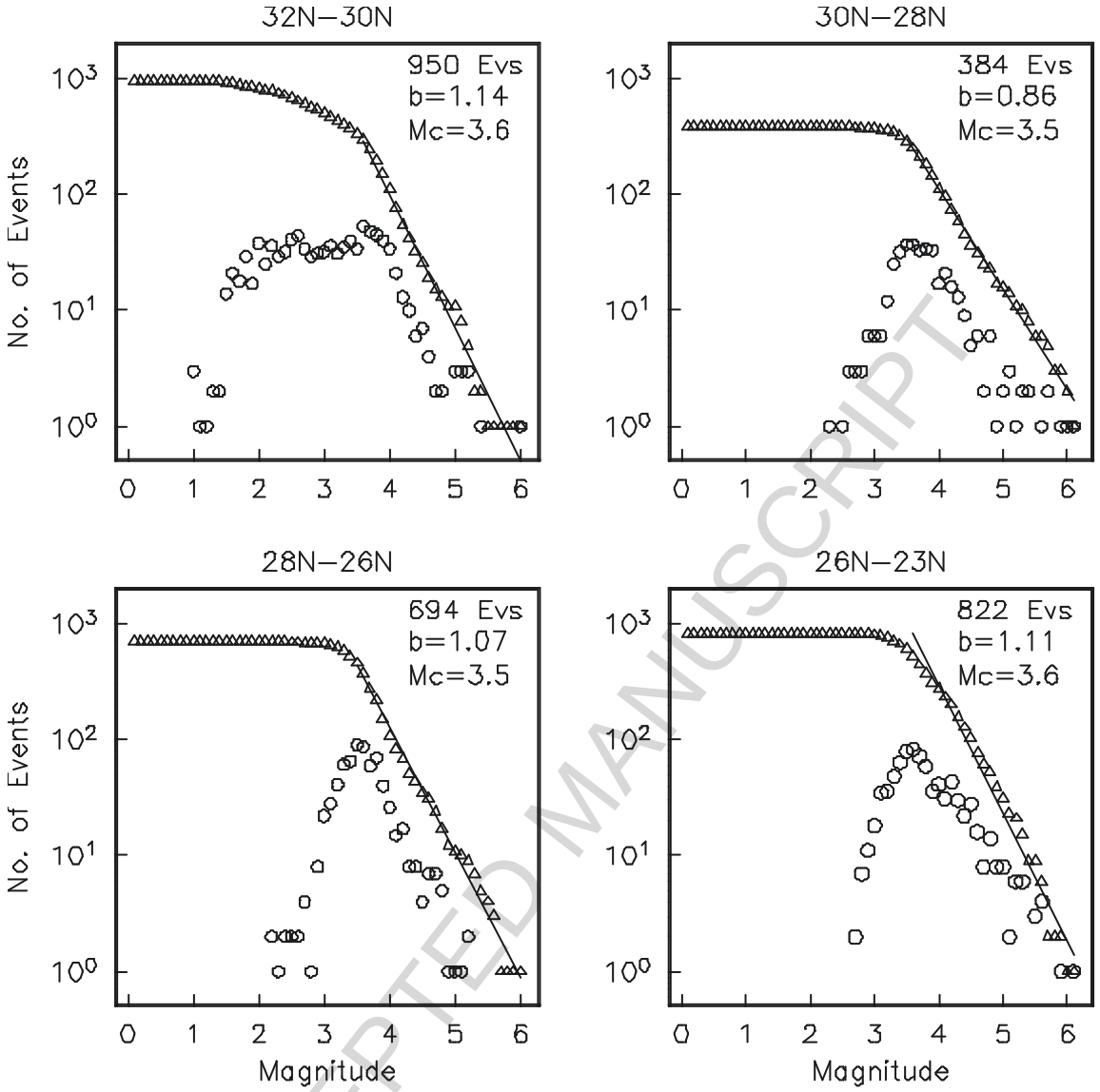

Figure 2. Minimum magnitude of completeness (*Mc*) and *b* value of the ISC catalog for earthquakes located in the GoC between 2002-04-01 and 2014-12-31. The cumulative frequency (triangles) and non-cumulative frequency (circles) from events in four regions of the GoC are displayed. Upper frames correspond to the northern Gulf (latitudes 30°-32°N and 28°-30°N) and bottom frames to the southern GoC (latitudes 26°-28°N and 23°-26°N).

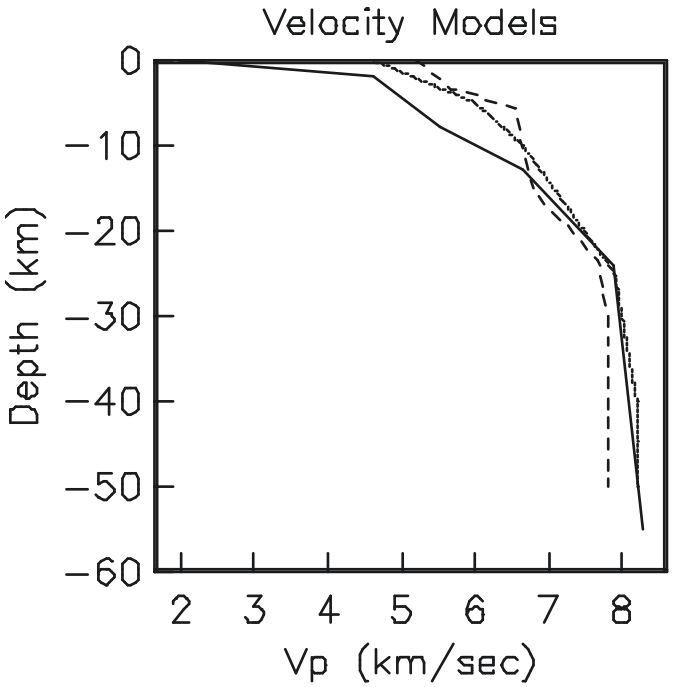

Figure 3. *P* wave velocity models used. The solid line is the model determined by Gonzalez-Fernandez *et al*., (2005), the dotted line is the model of Lopez-Pineda *et al*., (2007) and the dashed line the velocity model derived by Sumy *et al*. (2013).

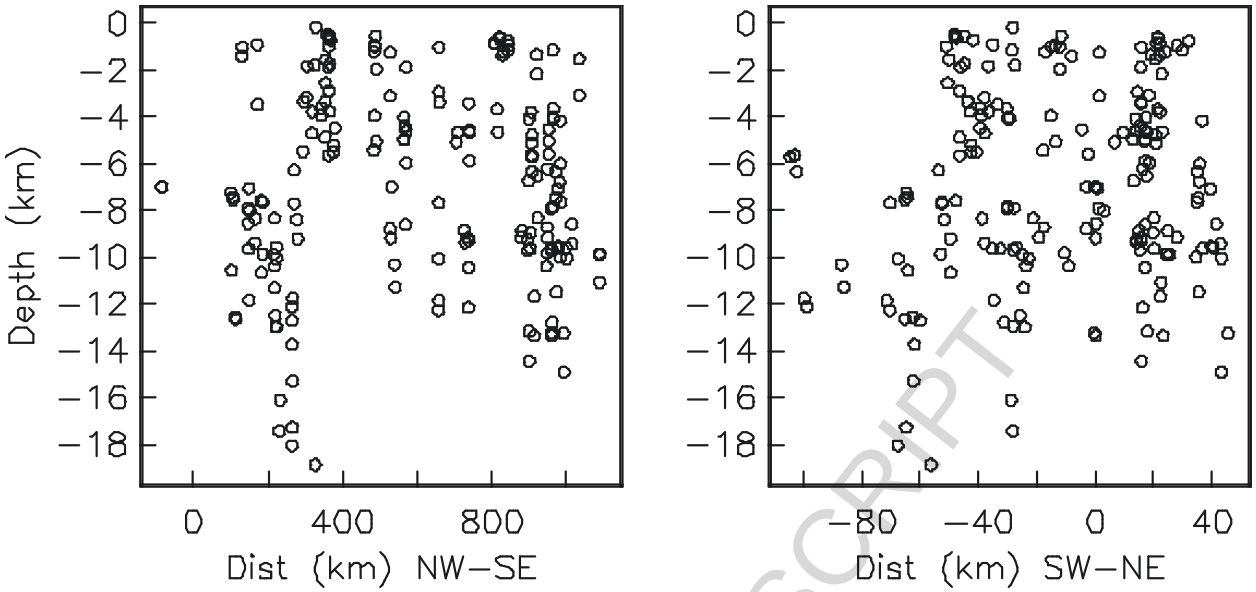

Figure 4. Cross sections using hypocenters relocated with the double-difference method. The left frame shows the distribution of the earthquakes projected on a plane parallel to the GoC axis (NW-SE direction) with the origin at the northernmost point of the gulf (31.786°N, 114.750°W) (profile A-A' in Fig. 1). The right frame displays the hypocenters projected on a plane perpendicular to the axis of the gulf, in the SW-NE direction (profile B-B' in Fig. 1). The vertical exaggeration is 60 times the horizontal scale.

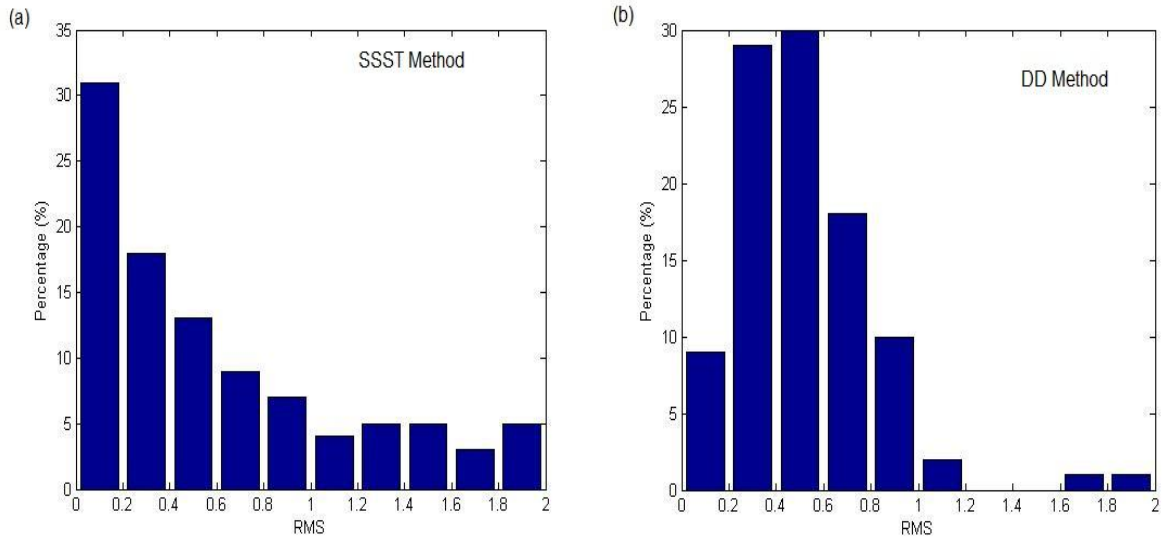

Figure 5. Root Mean Squares (RMS) of hypocenter location error versus the percentage of earthquakes located. (a) Using the Source Specific Station Term (SSST) method (Lin and Shearer, 2005). (b) Using the Double-Difference method (Waldhauser and Ellsworth, 2000). We did not include in the catalog any event with RMS>2.

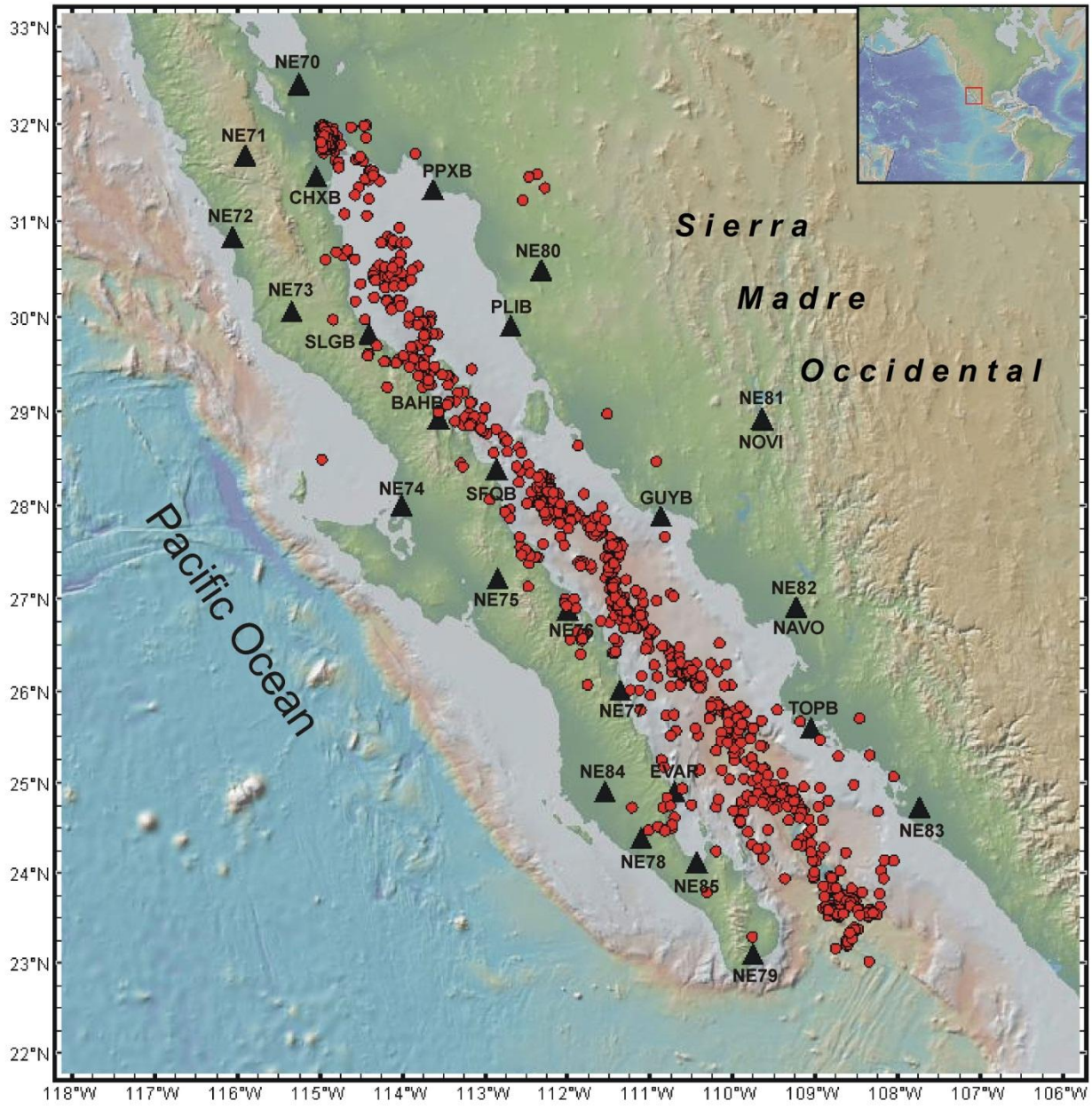

Figure 6. Location of epicenters (circles) listed in Table 1 of the electronic supplement. The topography and bathymetry are from GeoMap App.

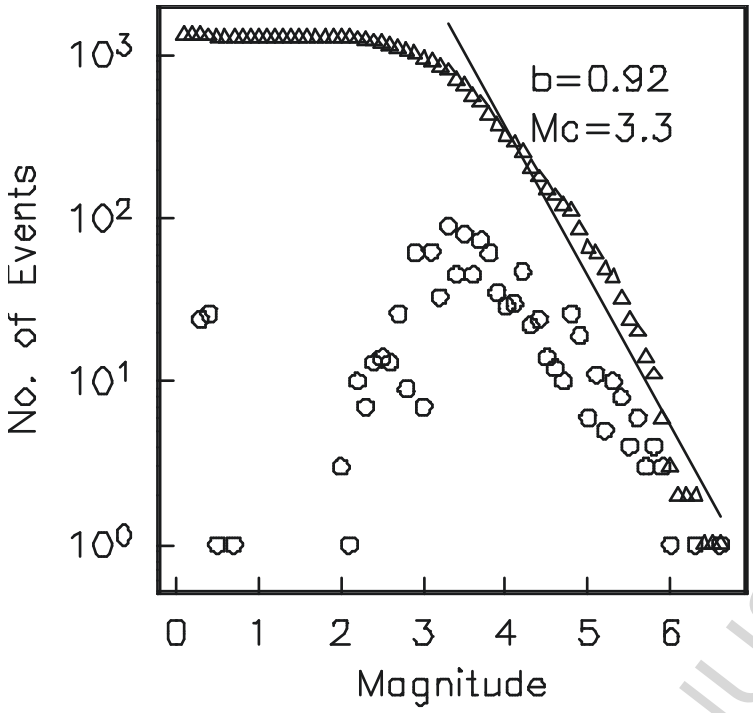

Figure 7. Minimum magnitude of completeness (*Mc*) and *b* value of the catalog of relocated earthquakes (shown in Fig. 6) in the GoC region between 2002 and 2014. The cumulative frequency (triangles) and non-cumulative frequency (circles) in the whole GoC region is displayed.

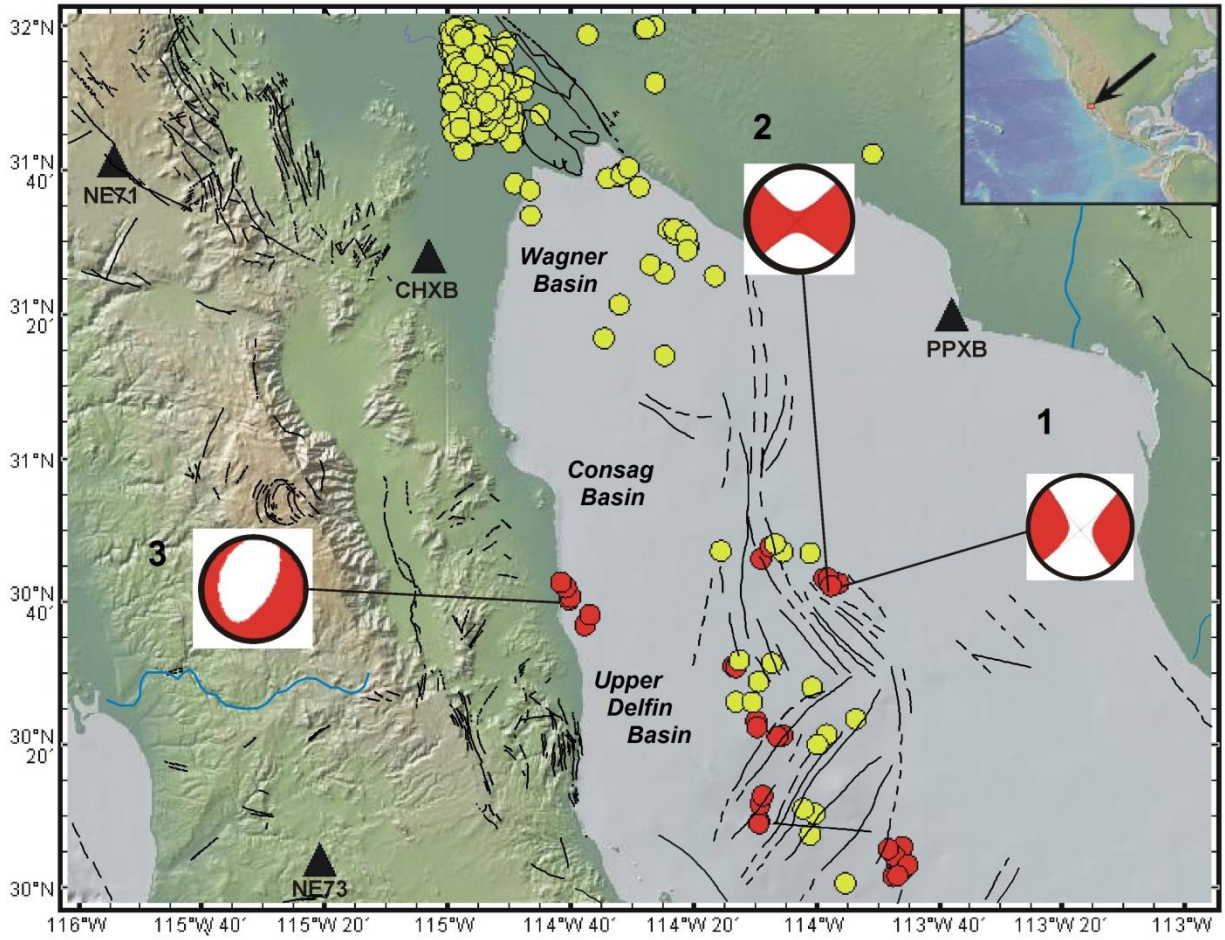

Figure 8. Epicenters relocated in the northernmost zone of the GoC, for the period 2002-2014. The red circles are earthquakes relocated with hypoDD (Waldhauser and Ellsworth, 2000) and the yellow circles are events from the 2011-Hauksson-Yang-Shearer, Waveform Relocated Earthquake Catalog for Southern California (Hauksson *et al*., 2012; Lin *et al*., 2007). The focal mechanisms were taken from the GCMT catalog and the faults from the Generic Mapping Tools (Wessel and Smith, 1998). The topography and bathymetry are from GeoMap App (Ryan *et al*., 2009)

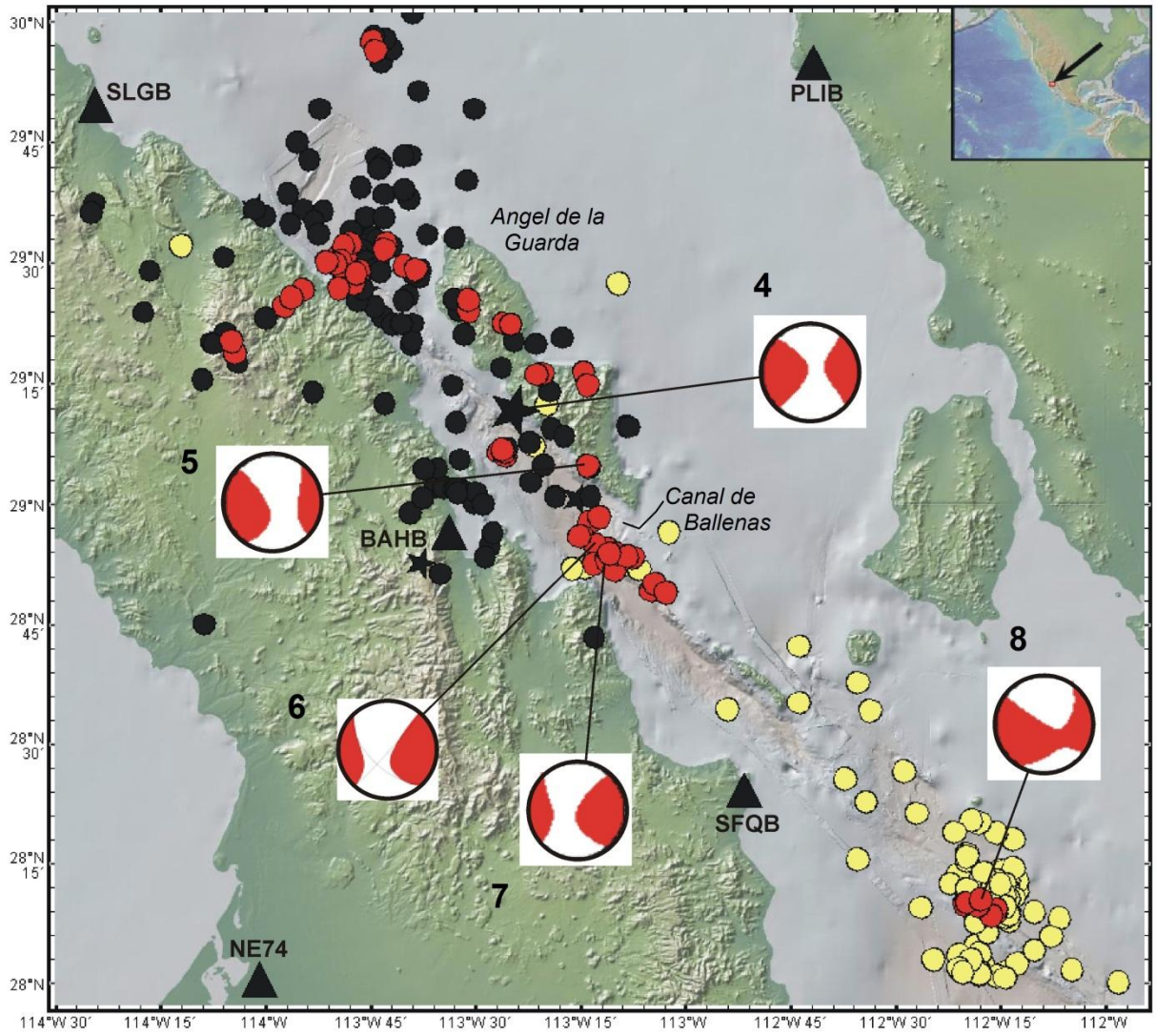

Figure 9. Epicenters relocated in the north-central zone of the GoC, for the period 2002-2014. The red circles are earthquakes relocated with hypoDD (Waldhauser and Ellsworth, 2000) and the yellow circles earthquakes relocated by Sumy *et al*., (2013) using the OBS of the SCOOBA experiment. Epicenters on black were located by Castro *et al*. (2011b) and the focal mechanisms were taken from the GCMT catalog. The topography and bathymetry are from GeoMap App.

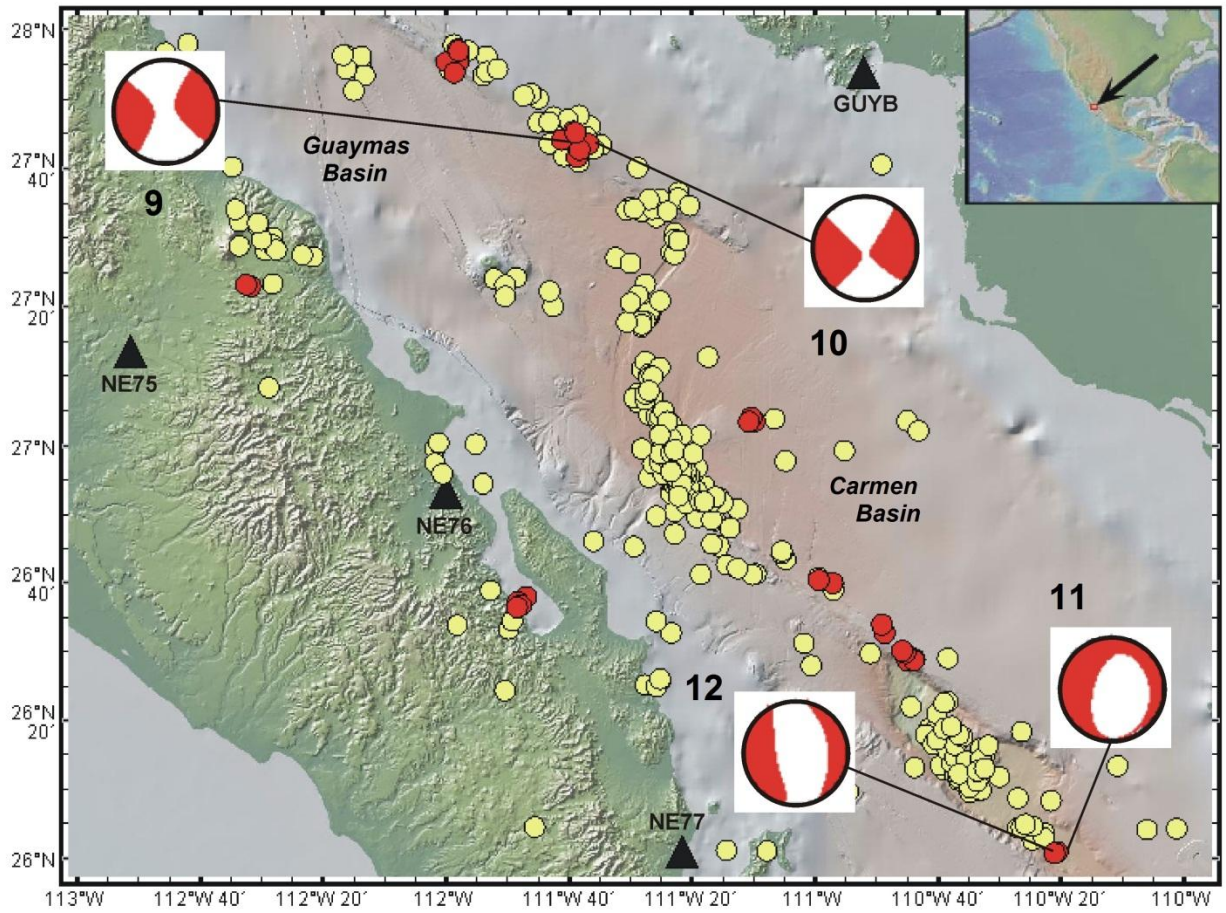

Figure 10. Epicenters relocated in the south-central zone of the GoC, for the period 2002-2014. The red circles are earthquakes relocated with hypoDD (Waldhauser and Ellsworth, 2000) and the yellow circles are events located by Sumy *et al*. (2013). The focal mechanisms were taken from the GCMT catalog. The topography and bathymetry are from GeoMap App.

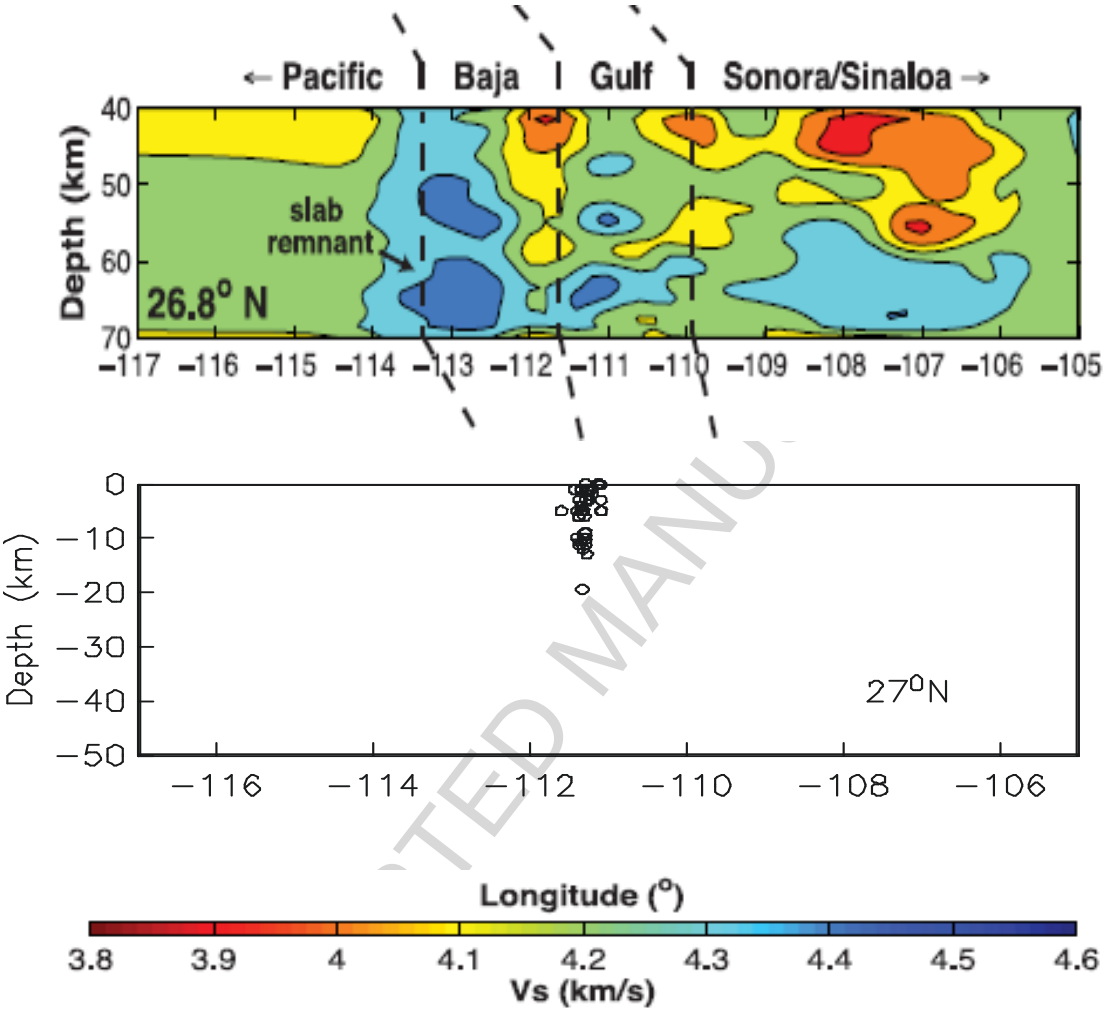

Figure 11. East-west profiles showing the average shear wave velocities (top), modified from Di Luccio *et al.*, (2014), and hypocenters relocated in this study between 26.9°N and 26.7°N.

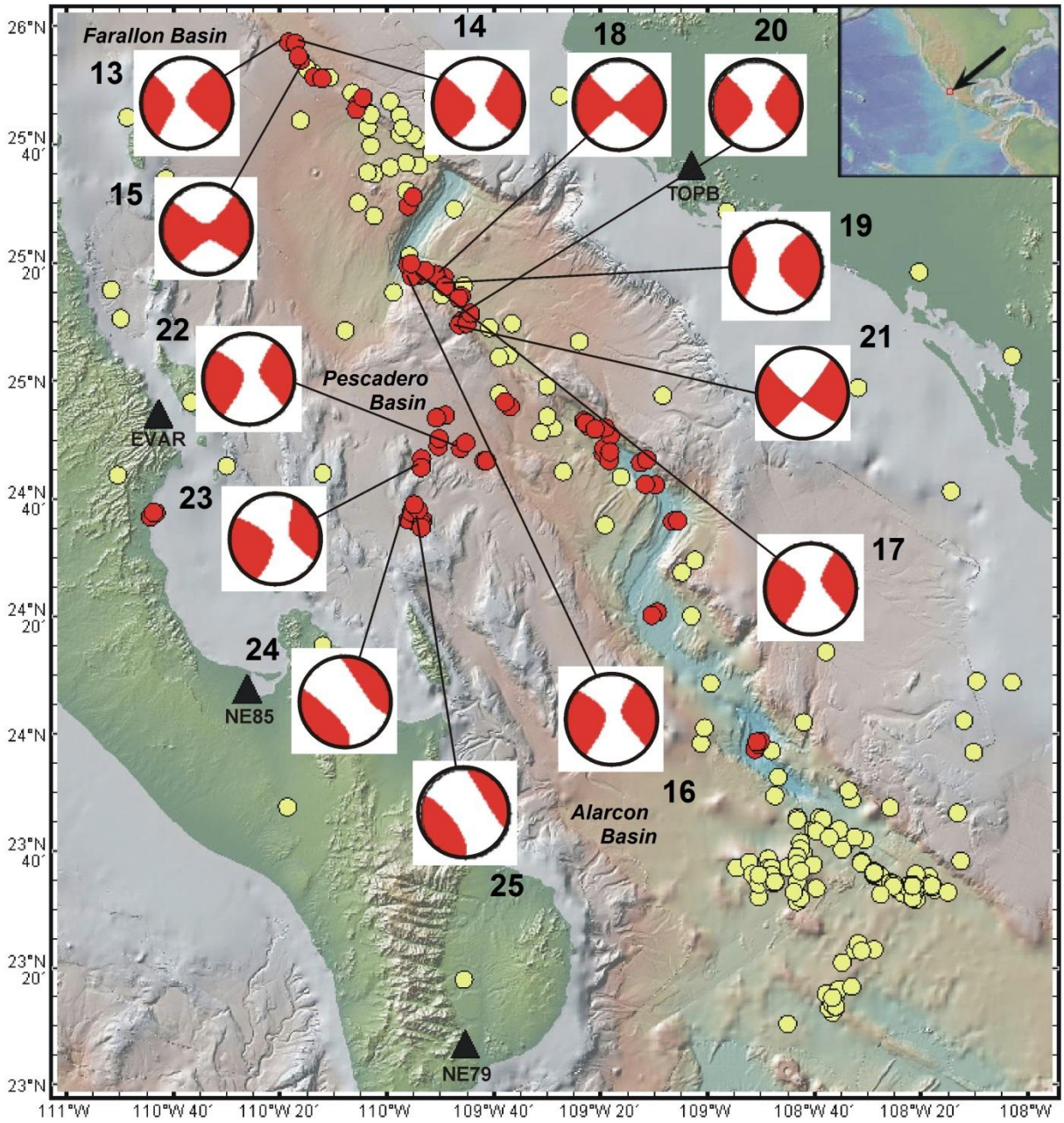

Figure 12. Epicenters relocated in the southern zone of the GoC, for the period 2002-2014. The red circles are earthquakes relocated with hypoDD (Waldhauser and Ellsworth, 2000) and the yellow circles are events located by Sumy *et al*. (2013). The focal mechanisms were taken from the GCMT catalog. The topography and bathymetry are from GeoMap App.

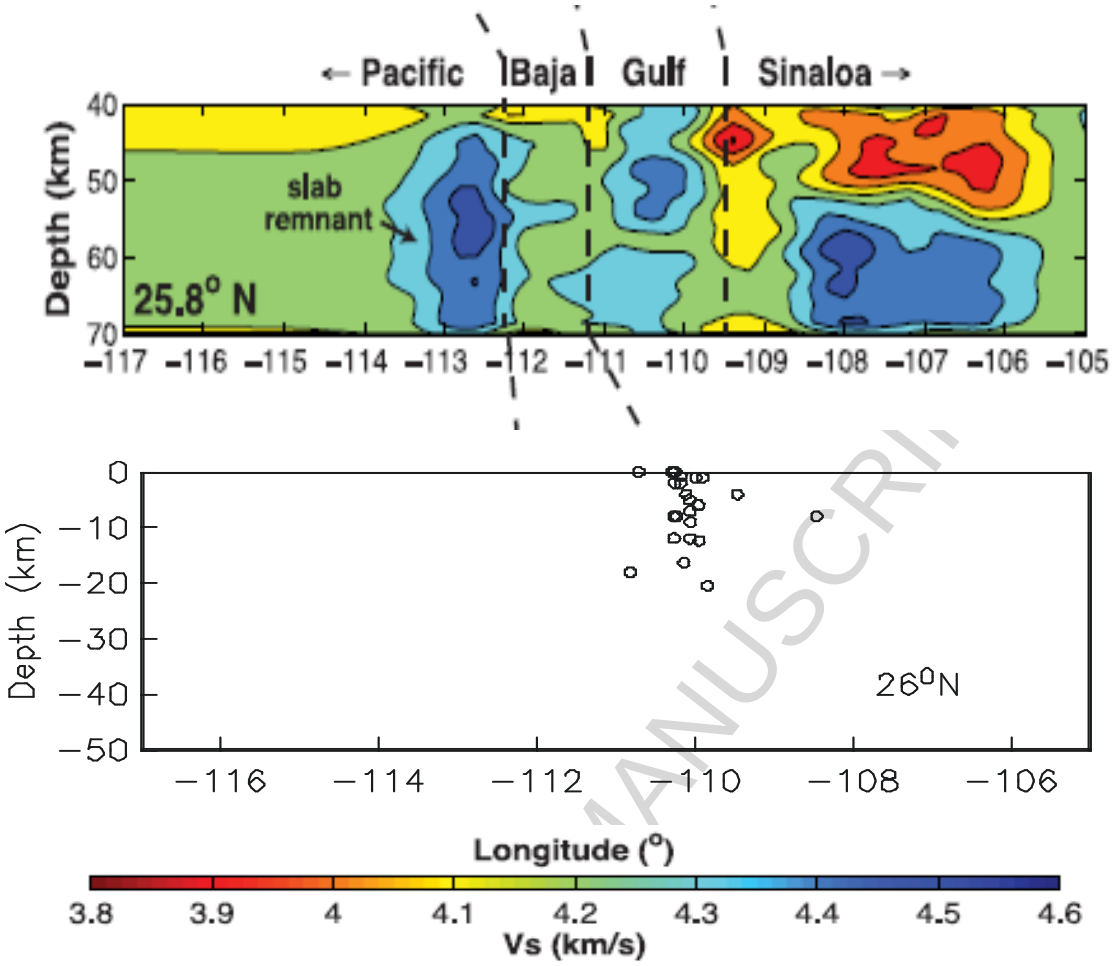

Figure 13. East-west profiles showing the average shear wave velocities (top), modified from Di Luccio *et al.*, (2014), and hypocenters relocated in this study between 25.7°N and 25.9°N.

Highlights of Manuscript TECTO-S-16-00620

"*Active Tectonics in the Gulf of California and Seismicity (M>3.0)*

for the Period 2002-2014"

By Castro, Stock, Hauksson and Clayton

- A catalog of earthquakes located in the Gulf of California (GoC), that permits to analyze the seismotectonics and depth of the seismogenic zone of this region, is presented.
- This well constrained catalog of seismicity highlights zones of active tectonics and seismic deformation within the North America-Pacific plate boundary.
- The minimum magnitude of completeness of this catalog is *Mc*=3.3and the *b* = 0.92±0.04 value of the Gutenberg-Richter relation.
- Most earthquakes in the southern GoC are generated by transform faults and this region is more active than the central GoC region.
- The northern region, where most deformation is generated by oblique faults, is as active as the southern region.
- Stress transfer outside the plate boundary, caused by geometrical irregularities and/or reactivation of preexisting faults, generates clustered swarms of intraplate earthquakes.